AGU ADVANCING EARTH AND SPACE SCIENCES

Water Resources Research

RESEARCH ARTICLE
10.1029/2025WR040216

Spatially Distributed Modeling of Lake Ice Trends and Distribution in the North Slave Region, NWT, Canada

G. Attiah[1,2], **K. A. Scott**[2,3], **and H. Kheyrollah Pour**[1,2]

[1]Department of Geography and Environmental Studies, ReSEC Research Group, Wilfrid Laurier University, Waterloo, ON, Canada, [2]Cold Regions Research Centre, Wilfrid Laurier University, Waterloo, ON, Canada, [3]Department of Mechanical and Mechatronics Engineering, University of Waterloo, Waterloo, ON, Canada

Key Points:

- Distributed lake ice model at a ~50 m resolution for predominantly small to medium lakes using satellite and reanalysis data as inputs
- The modeled lake ice thickness agrees with the in situ data collected from the field, with a root mean squared error from 2.7 to 7 cm
- Decline in ice thickness (−0.26 to −0.10 cm/year) and duration (−0.40 to −0.15 days/year) across 500 lakes in the Northwest Territories

Correspondence to:
G. Attiah,
gattiah@wlu.ca

Citation:
Attiah, G., Scott, K. A., & Kheyrollah Pour, H. (2025). Spatially distributed modeling of lake ice trends and distribution in the north slave region, NWT, Canada. *Water Resources Research*, *61*, e2025WR040216. https://doi.org/10.1029/2025WR040216

Received 12 FEB 2025
Accepted 7 SEP 2025

Author Contributions:
Conceptualization: G. Attiah, K. A. Scott, H. Kheyrollah Pour
Data curation: G. Attiah
Formal analysis: G. Attiah
Funding acquisition: K. A. Scott, H. Kheyrollah Pour
Investigation: G. Attiah
Methodology: G. Attiah, K. A. Scott, H. Kheyrollah Pour
Project administration: H. Kheyrollah Pour
Resources: K. A. Scott, H. Kheyrollah Pour
Software: G. Attiah
Supervision: K. A. Scott, H. Kheyrollah Pour
Validation: G. Attiah
Visualization: G. Attiah
Writing – original draft: G. Attiah
Writing – review & editing: G. Attiah, K. A. Scott, H. Kheyrollah Pour

Abstract The Canadian Lake Ice Model has been adapted and distributed at a high spatial resolution (~50 m) to simulate Lake Ice Thickness (LIT) and phenology across small to medium-sized lakes in this study. The model was applied to simulate the spatial variability of LIT, Ice Cover Duration (ICD), and Lake Ice Phenology across 500 predominantly small to medium-sized lakes in the North Slave Region (NSR) of the Northwest Territories (NWT), Canada, from 1984 to 2022. The model utilizes a 30 m grid lake surface temperature (LST) data set derived from the North Slave LST data set, along with climate inputs from the European Center for Medium-Range Weather Forecasts Reanalysis v5 (ERA5), including wind speed, relative humidity, snowfall, and cloud cover. These inputs provide surface fluxes to the model, driving its unsteady heat equation to produce daily LIT, annual ICD, and annual freeze-up and break-up dates on a ~50 m grid resolution. Validation against in situ measurements shows a root mean square deviation of 2.7–7 cm for LIT. Trend analysis revealed a significant decline in LIT (−0.26 cm/year to −0.10 cm/year) and ICD (−0.40 days/year to −0.15 days/year). The highest rates of LIT decline are observed in the early and later months of ice formation. Freeze-up timings are primarily influenced by depth, while geographic factors such as latitude and elevation affect break-up timing in the NSR. This distributed modeling approach provides a robust assessment of lake ice variability and trends under changing climate and weather conditions.

Plain Language Summary Satellite-derived lake surface temperature data from the North Slave Region (NSR) and weather data from ERA5 were used to model how ice thickness changes across lakes over time. By applying a lake ice model at a high resolution (~50 m), we were able to estimate daily ice thickness, when lakes freeze and melt, as well as how long ice persists on a lake, from 1984 to 2022 for 500 lakes in the NSR of the Northwest Territories, Canada. The model performed well, with ice thickness estimates differing from real-world measurements by only 2.7–7 cm. Over nearly four decades, the results showed that ice is thinner (losing 0.10–0.26 cm per year), and ice cover duration is getting shorter (shrinking by 0.15–0.40 days per year). Freeze-up timing were mainly influenced by lake depth, while break-up was more affected by the lake's location and altitude.

1. Introduction

Warming in Arctic regions since the late 1970s is reported to be almost four times that of the global rate (Rantanen et al., 2022) and has impacted several components of the Earth's cryosphere. As global temperatures continue to rise, there are implications for Northern Canada, whose socioeconomic and cultural systems are centered around ice and snow and where changing lake ice regimes are linked to the natural resource industry (Knoll et al., 2019; Mullan et al., 2017; T. D. Prowse et al., 2009). Communities rely on freshwater ice to transport resources and people, forming an essential part of their infrastructure. Information on lake ice thickness (LIT), Ice Cover Duration (ICD), and Lake Ice Phenology (LIP) are crucial for planning and constructing safe winter roads for transportation. In the Northwest Territories (NWT), Canada, winter roads are critical to their economy, with yearly transportation of over $500 million worth of goods on winter roads like the Tibbitt to Contwoyto Winter Road (TCWR) (Mullan et al., 2017).

In addition to its critical importance for the infrastructure of Northern communities, lake ice has been recognized as an Essential Climate Variable by the Global Observing System and the World Meteorological Organization because of its significance in understanding climate change and its potential for long-term monitoring. Furthermore, lake ice plays a vital role in the physical, biological, and chemical processes of freshwater in cold

regions. LIP (duration, freeze-up, and break-up dates) has proven to be a strong indicator of climate change and its variability (Brown & Duguay, 2011), since regional weather patterns are interconnected with lake ice processes (Brown & Duguay, 2010).

Increased climate warming significantly impacts lake ice regimes, leading to higher water temperatures, thinner ice, later freeze-up dates, and earlier break-up dates (Dibike et al., 2011; Hampton et al., 2024; Weyhenmeyer et al., 2022). Early ice break-up dates due to these changes enhance the absorption of solar radiation, thereby affecting energy and moisture exchanges (Ménard et al., 2002; Slater et al., 2021; W. Wang et al., 2018). Changes in LIP impact the ecology, temperature distribution, stratification, and water levels of lakes (Dibike et al., 2011; Hampton et al., 2017). Furthermore, regional variations in the phenology of lake ice may impact the energy and water balances of landscapes, affecting hydrological processes (e.g., sediment and nutrient fluxes, river flow regimes) and aquatic habitats (Prowse et al., 2011). Studies have reported increased lake temperatures with decreased seasonal ICD (Attiah et al., 2023a; Lehnherr et al., 2018; O'Reilly et al., 2015; Šmejkalová et al., 2016), which is expected to continue (Brown & Duguay, 2011; Post et al., 2019). Therefore, continuous monitoring of LIT, ICD, and LIP is crucial for understanding how lakes respond to a changing climate.

Research has revealed that, despite shared warming patterns across regions, individual lake behavior and properties impact the rate of their respective ice cover loss, and this information is vital for future projections and modeling of lake ice changes (Arp et al., 2013; Liston & Dorothy, 1995; Warne et al., 2020). However, collecting in situ data for lake ice monitoring on individual lakes is challenging, especially in the subarctic shield. Firstly, harsh weather, eco-environmental conditions, and remoteness curtail continuous in situ measurements of lake ice conditions (Qiu et al., 2019). Secondly, it is prohibitively time-consuming, destructive, and costly, especially for long-term daily lake ice monitoring (Matsumoto et al., 2019). Additionally, using weather station data as input in models to monitor lake ice can prove challenging due to their sparse distribution, especially in regions such as the North Slave Region (NSR) in the NWT. Furthermore, the spatial representation of lakes is limited when relying on in situ measurements and weather station data (Kämäri et al., 2017). Such data typically represent conditions at a single point, specific parts of a lake, or a nearby station, failing to capture processes on the entire spatial extent of the lake. These logistical challenges lead to reduced data collection, incomplete data sets, and selective monitoring.

Satellite optical and thermal remote sensing has become a powerful tool for monitoring ICD and LIP (Dastour et al., 2022; Guo et al., 2021). Its importance has grown in recent years, particularly in regions where ground-based observational networks have become limited or unavailable. However, a key limitation of multispectral remote sensing in lake ice research is its inability to directly measure LIT, as this is a subsurface feature.

Spatially distributing a thermodynamic lake ice model using gridded reanalysis and satellite data as input provides an effective solution to these limitations. Using satellite data as forcing instead of in situ and/or weather station data, the model can simultaneously simulate ice conditions across the entire lake. Furthermore, spatially distributed models enable broader applications in lake ice research by incorporating intra-lake spatial variability (Huss & Farinotti, 2012; Spence et al., 2011). This approach is particularly crucial for lake ice simulation, as the climate variables influencing lake ice are inherently spatially and temporally variable.

In this study, the CLIMoGrid model (Canadian Lake Ice Model-Grid) is adapted and enhanced to run at a fine spatial resolution of 0.0005° (∼50 m) for simulating LIT, ICD, and LIP on small to medium-sized lakes. The model is applied to 500 lakes of varying sizes in the NSR of the NWT, Canada, over an extensive period from 1984 to 2022. By simulating LIT on each ∼50 m grid cell, this study effectively captures and visualizes spatial variations in LIT, providing a robust foundation for investigating the factors driving these variations. Additionally, incorporating lakes with diverse characteristics such as size, depth, and geographic location allows for the monitoring and analysis of both intra- and inter-lake variability of LIT. This approach provides a deeper understanding of the underlying processes governing ice formation and development in different lake environments. In addition to simulating LIT, the model's capability to simulate ICD and LIP enables a comprehensive analysis of the ice phenology over the study period. Model outputs are compared with observed data from field studies for validation and calibration to ensure the accuracy and reliability of the simulated results.

10.1029/2025WR040216

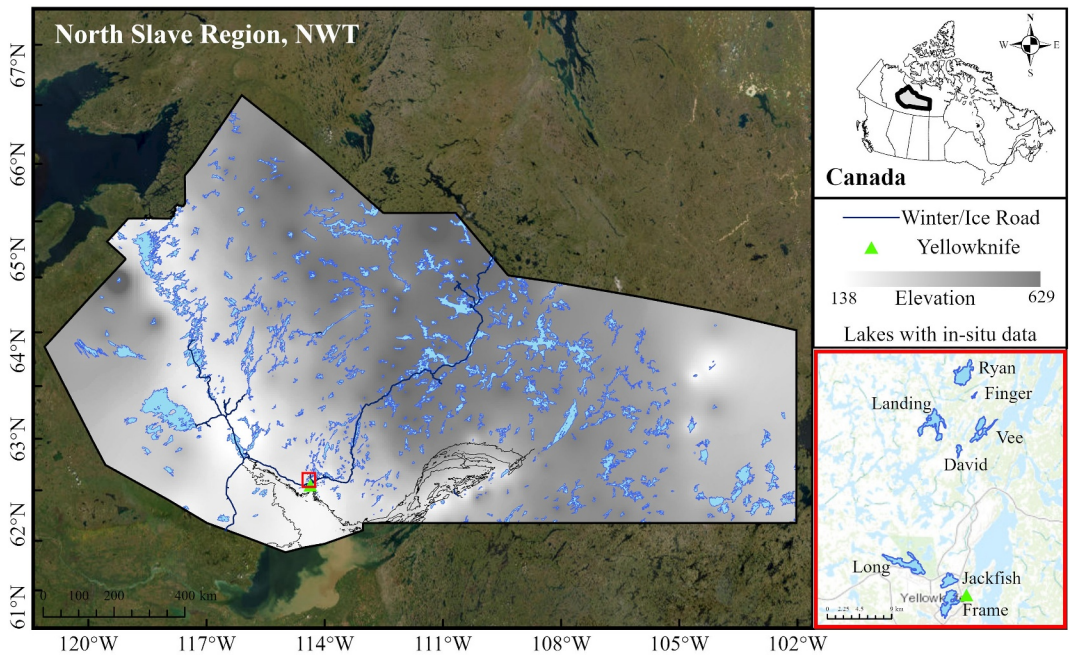

Figure 1. Geographical distribution of study lakes in the North Slave Region of Canada's Northwest Territories. Highlighted lakes indicate the locations where fieldwork was conducted.

2. Materials and Methods

2.1. Study Lakes

This study focuses on NSR within NWT, Canada (Figure 1), spanning approximately 61.68°–66.84°N and −121.24° to −102.00°E. This region covers a vast area of ∼316,000 km^2, situated in the Slave province of the Canadian Shield. The NSR is characterized by a diverse landscape and an average elevation of 301 m. The climate in this region exhibits a wide temperature range, with extreme lows around −40°C and summer highs reaching up to 25°C. With over 10,000 lakes, the NSR is a remarkable example of a region that is densely populated with lakes, containing ∼38% of the lakes in NWT (Messager et al., 2016). These lakes vary in size and depth, with the most notable feature being the East Arm of the Great Slave Lake, which reaches an impressive depth of 614 m. The NSR is also the most densely populated administrative area within the NWT. Additionally, the region boasts one of the longest winter roads globally, the Tibbitt TCWR, spanning ∼600 km and serves as a vital transportation route across frozen lakes and tundra.

LIT, ICD, and LIP were simulated for 500 lakes in this region. Most of the lakes studied (22%) had a surface area below 5 km^2. The distribution of lake surface areas is as follows: 12 % for lakes over 1 km^2, 22% for lakes between 1 and 5 km^2, 12% for lakes between 5 and 10 km^2, 21% for lakes between 10 and 25 km^2, 13% for lakes between 25 and 50 km^2, 10% for lakes between 50 and 100 km^2, and 10% for lakes over 100 km^2. The distribution of lake depths was 27% for depths of 1–5 m, 38% for 5–10 m, 30% for 10–25 m, and 5% for depths over 25 m.

2.2. Data Sources

2.2.1. Field Measurements and Observations

Field-based in situ LIT measurements were used as a validation data source. LIT data were collected using an ice auger and a tape measure. Measurements (265) were conducted on eight study lakes: David, Ryan, Landing, Frame, Jackfish, Long, Finger, and Vee Lakes (Figure 1). Data were collected over 12 days between November 24 and 14 December 2021. The second source of in situ data for validation was LIT measurements obtained from Snow and Ice Mass Balance Apparatus (SIMBA) sensors deployed on two of the study lakes, Ryan and Landing lakes, from December 2021 to March 2022. The SIMBAs were equipped with thermistor chains, 3–5 m in length, containing ambient temperature sensors spaced every 3 cm, extending from the air through the snow and ice and

into the water. These sensors recorded temperatures at 15-min intervals. LIT was derived from SIMBA measurements based on the differences in thermal properties of water, ice, snow, and air, as described by Rafat et al. (2023). For this study, the maximum daily LITs retrieved from the SIMBAs were compared to model outputs for validation. These in situ measurements were compared to LIT values derived from CLIMoGrid simulations at a ∼50-m grid resolution.

2.2.2. Gridded Lake Surface Temperature Data

Lake surface temperature (LST) data was derived from the North Slave LST satellite-derived data product, with European Centre for Medium-Range Weather Forecasts Reanalysis v5 (ECMWF ERA5-Land) reanalysis data used to fill gaps in the data. The North Slave LST is an open-access gridded data set (https://doi.org/10.5683/SP3/J4GMC2) providing the spatial distribution of LST on lakes in the NSR, NWT, Canada, since 1984, at a ∼30 m grid resolution (Attiah et al., 2022). The data set was generated using the thermal bands of Landsat-5 TM, Landsat-7 ETM+, and Landsat-8 OLI/TIRS using a single-channel retrieval algorithm. LST values in the data set have been buffered to minimize the effect of lake pixels mixing with the land, and cloud cover has been eliminated from the data. LST data shows a good agreement (RMSD = 1.71°C) with in situ measurements described by Attiah et al. (2023b).

The ERA5-Land reanalysis data set provides decades of data on the evolution of variables on the Earth's surface at a ∼9 km spatial resolution (Sabater, 2019). This data set is an optimal combination of observations and model data based on physical laws, generating continuous, consistent data that provides information on the changing climate. For this study, the LST of ERA5-Land hourly data was used, representing the Earth's uppermost surface (skin) temperature. Air temperature is estimated using surface temperature from North Slave LST and ERA-Land by applying the following equation (Wang et al., 2010):

$$T_a = LST + \delta T \tag{1}$$

where δT is a function of the cloud fraction, which under clear-sky conditions is ∼2.2°C (Persson et al., 2002) and is set here as:

$$\delta T = 2.2 - 1.8C_f \tag{2}$$

where C_f is the cloud fraction ranging from 0 to 1 derived from ERA5.

2.2.3. Gridded Data for Other Climate Variables

ECMWF ERA5 reanalysis data was used to extract climate variables, including wind speed (m s-1), relative humidity (%), snow fall (m), and cloud cover from 1984 to 2022. ERA5 is the fifth generation of climate reanalysis data (Hersbach et al., 2020), providing atmospheric, land, and oceanic variables. Relative humidity was derived from ERA5 hourly data on pressure levels (upper air fields), while the other variables were obtained from ERA5 hourly data on single levels (atmospheric, ocean-wave, and land surface quantities). ERA5 data have a spatial resolution of ∼30 km and a temporal resolution of 1 hour.

2.3. Lake Ice Model and Data Integration

This study uses the CLIMoGrid model, a spatially distributed model adapted from the one-dimensional (1-D) thermodynamic lake ice model CLIMo (Duguay et al., 2003). CLIMoGrid was initially developed to simulate LIT, ICD, and LIP for large northern lakes, such as Great Bear Lake and Great Slave Lake (Kheyrollah Pour et al., 2024), at a spatial resolution of 1 km. This study improves upon CLIMoGrid by enhancing and adapting it for small to medium-sized lakes with a finer spatial resolution (∼50 m). It incorporates updated algorithms and inputs tailored to smaller lakes with diverse characteristics. This improved version of CLIMoGrid ensures robust and accurate simulations by integrating data from multiple sources and addressing spatial heterogeneity in lake and climate characteristics. Lake-specific parameters, such as snow density and mixing depth, were incorporated to refine the simulations and enhance the model's capability to represent ice dynamics in smaller, more spatially complex lake environments. To run the enhanced CLIMoGrid, a Python module has been developed, which solves the unsteady heat conduction equation at each pixel on a given lake. The first function in the module allows

users to input specific parameters and specifications to run the model effectively. These parameters include the start and end date specification for simulations, the bounding geometry or shapefile of the lake area to be simulated, the dry and wet snow density, mixing depth, and snow retention percentage on the lake.

The model packages the data for the specified years and location (lake area) based on user inputs. For each given lake, the model will generate a 0.0005° grid across the spatial extent specified to fill with model inputs and outputs. Snowfall, humidity, cloud cover, and wind values for each pixel were extracted from ERA5 data and filled with station data when absent. The LST corresponding to each pixel location is first retrieved from the North Slave LST for a particular day. In the absence of this data, LST is extracted from ERA5-Land to fill in missing values, as this data set had the closest values compared to the North Slave LST. This process ensures daily temperature, snow, humidity, cloud, and wind values for each grid on the lake within the studied ice season (1984–2022). LIT is calculated on each pixel across the lakes for the entire study period, with the data and inputs created. The model spins up twice over the first year to ensure that some pseudo-previous data exists to run the model.

2.4. Simulation of Ice Thickness

In this study, simulations were conducted using a 75% snow cover scenario to represent snow retention on the ice surface. Based on data collected in the field, the density for dry snow was set at 250 g/cm^3, and the density for wet snow was set at 300 g/cm^3. The lake's mixing depth was calculated based on lake area and depth information, with equations derived from Cruikshank (1984):

$$\text{Mixing Depth} = \frac{1.98 \times \text{Depth}^{0.47} + 2.76 \times \text{Area}^{0.21}}{2} \quad (3)$$

where area (km^2) and depth (m) are retrieved from the HydroLAKES database.

The shapefile of lakes were provided as inputs to ensure that simulations were constrained within lake boundaries. The data was split into 0.05° × 0.05° bins to enable parallel processing, which were subsequently merged to reduce computational run times. For a given lake, an output NetCDF file was generated containing the following variables: daily LIT values (in meters), annual freeze-up, and break-up dates (in the day of the year, DOY) across the lake defined spatial extent. Figure 2 summarizes the workflow and data used for the LIT simulation.

2.5. Lake Trend Analysis and Correlation

A 3 × 3 group of pixels at the centroid within the lake was extracted to examine the daily transition of LIT, ICD, and LIP from 1984 to 2022 to assess ice cover trends. Time series data were generated from the gridded NetCDF files for further trend, distribution, and correlation analysis. Daily maximum, minimum, and mean of LIT and annual LIP dates were extracted. Ice Cover Duration was calculated from the LIP dates, and long-term trends for LIT, ICD, and LIP were analyzed using the Mann-Kendall test. The null hypothesis (H0) assumed no trend, while the alternative (Ha) indicated either a decreasing or increasing trend (Kendall, 1975). Trend significance was evaluated at $p < 0.05$ unless stated otherwise.

Climate and morphometric parameters were compared with the simulated LIT to identify the primary drivers of LIT across the study area. The parameters included latitude, longitude, elevation, area, depth, and volume. Latitude and longitude were extracted from the centroids of lake polygons, which were automatically generated using the polygons. Lake elevation and depth were obtained from the HydroLAKES database (Messager et al., 2016). The lake area was calculated and generated using the lake shoreline shapefiles in ArcGIS Pro.

3. Results

3.1. Model Validation

3.1.1. Comparison Between Simulated Ice Thickness and In-Situ Measurements

In situ LIT measurements from 8 lakes in the NSR, NWT, were compared to the simulated LIT. Measurements were collected over 12 days between November 24 and 14 December 2021, and the location of the collected in situ data is shown in Figure 3. The mean absolute error for each in situ location ranged from 0 to 10 cm. Vee Lake

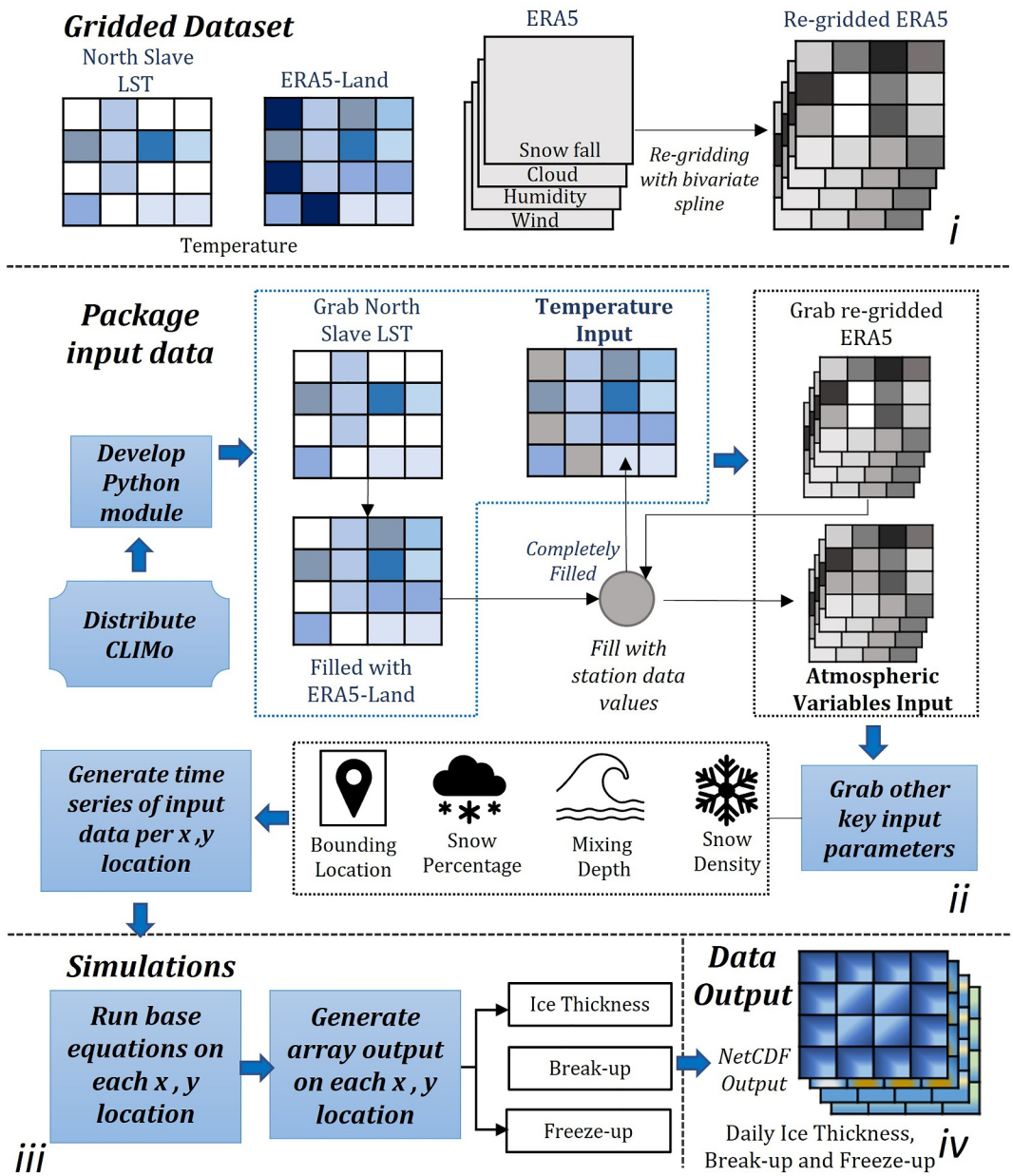

Figure 2. Workflow and data for simulating lake ice thickness and phenology.

has the lowest RMSE (2.7 cm) compared to the others, while Jackfish Lake showed the highest of 7 cm. The comparison between model-simulated LIT and in situ data across all 8 lakes revealed a good agreement, with an RMSE of 5.1 cm and an MBE of 2.3 cm. Analysis of the results on multiple lakes with different properties demonstrates the model's capability to simulate LIT across diverse lake conditions. However, divergences between the simulated LIT and field measurements are evident. The model overestimates LIT, particularly on parts of the lake with higher observed snow depths, as snow is a thermal insulator which slows ice growth. The model may not fully capture localized factors, such as the spatial heterogeneity of snow distribution and local wind patterns, leading to deviations from the in situ measurements. Despite these disparities, there are locations where the model and field data demonstrate good agreement, suggesting the model's capability to capture the overall spatial variations in LIT.

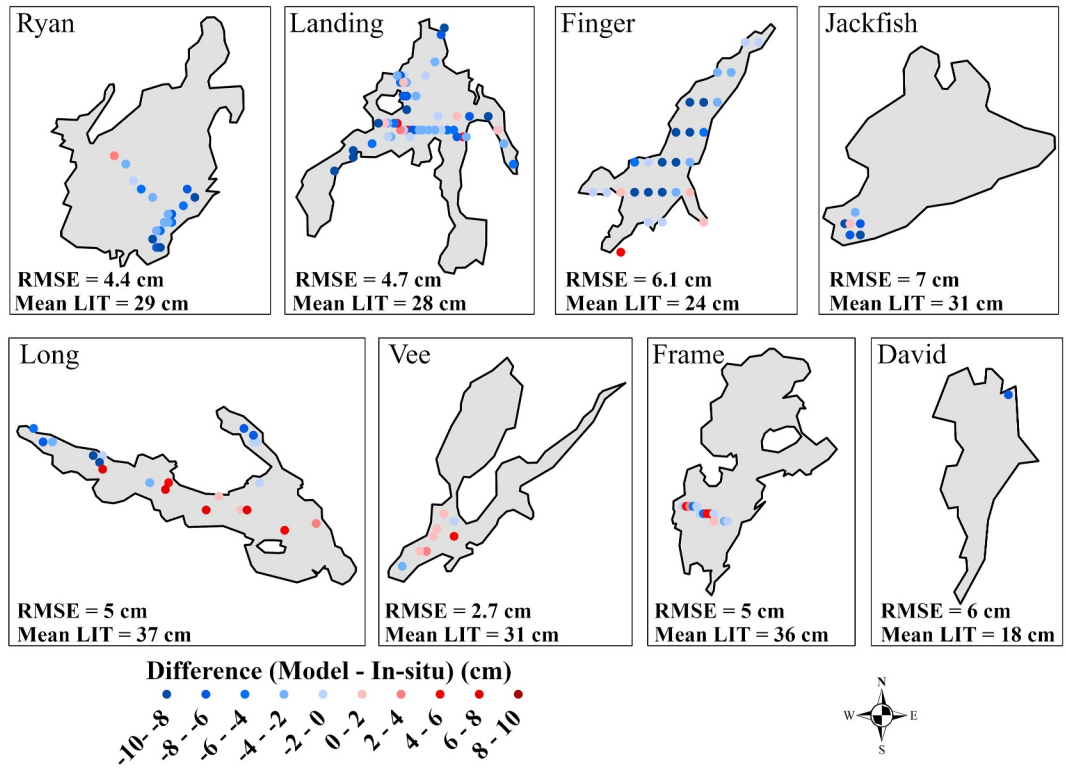

Figure 3. The location of collected in situ Lake Ice Thickness (LIT) measurements on 8 lakes (Figure 1) in the North Slave Region. Data was collected from across 12 days from November–December 2021. Differences between in situ and simulated ice thickness are represented in color. The mean LIT and RMSE for each lake is also shown.

3.1.2. Simulated Ice Thickness Compared to Snow and Ice Mass Balance Apparatus Values

The comparison between simulated LIT and measurements from SIMBA sensors provides a valuable quantitative evaluation of the model's temporal performance. Figure 4 shows the time series comparison of LIT derived from SIMBA and the model outputs for Ryan and Landing Lakes from January–March 2022. The model demonstrates good agreement with the SIMBA-derived LIT, with an RMSE of 4.66 cm, MBE of −3.63 cm and R^2 of 0.85 for Ryan Lake and RMSE of 6.24 cm, MBE of −5.83 cm, and R^2 of 0.51 for Landing Lake. This level of agreement aligns with the in situ data comparison presented in Section 3.1.1. The overall trend of increasing LIT over time is well captured by the model. There is a bias (underestimate) at both lakes earlier in the ice season. This underestimation may be attributed to uncertainties in the model's parameterizations, such as snow retention on the surface and fixed snow density, as well as assumptions regarding external influences on ice growth processes. Even though there are discrepancies, the model captures the general patterns of LIT growth, demonstrating its usefulness for understanding and predicting temporal changes in LIT.

3.2. Sample Model Output for a Given Lake

Trends and patterns in LIT and LIP are analyzed from the model output for a given lake. Agassiz Lake was selected as a case study, as it represents a typical medium-sized lake, to demonstrate an example of the information that can be derived from model outputs. Figure 5 shows sample outputs of LIT/LIP data and analysis on Agassiz Lake derived from model simulations. Daily ice thickness can be plotted for any single point on a lake over the entire study period. Figure 5.5a shows the daily LIT for a single point on Agassiz Lake for the 1991–1992 and 2021–2022 ice cover seasons. With this, the freeze-up date, break-up date, and ICD can be retrieved for both seasons for this single point on the lake. For this example, freeze-up occurs on October 19 for the 1991–1992 ice season and November 11 for 2021–2022. On the other hand, the break-up occurred on June 7 for the former ice season and May 29 for the latter. With these two dates, ICD can be calculated for both seasons, revealing 232 and

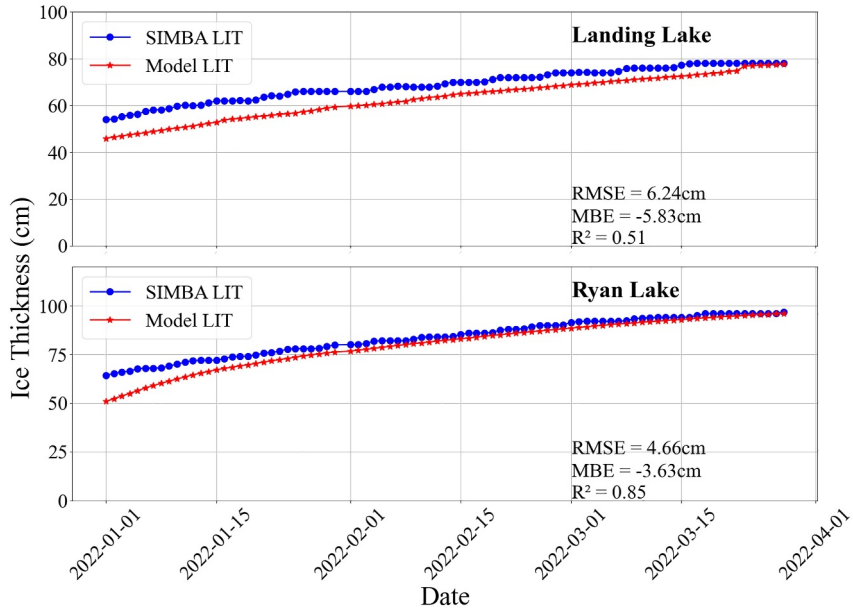

Figure 4. Time series comparison of the lake ice thickness derived from the Snow and Ice Mass Balance Apparatus measurements and model outputs for Landing and Ryan Lake between January and March 2022.

200 days for 1991–1992 and 2021–2022, respectively, indicating a 32-day decrease in ICD for the recent ice cover season due to its relatively late freeze-up.

In addition to the seasonal outlook of ice cover, yearly analysis can also be retrieved. Yearly mean LIT for the respective years can be analyzed to observe the trend (Figure 5b). Results for Agassiz Lake showed variability in the yearly LIT mean, which indicated a 0.1 cm/year reduction from 1984 to 2022. Additionally, annual LIP changes on a lake over the past 38 years can be examined. Each year's freeze-up and break-up day can be plotted (Figure 5c). Agassiz Lake showed an increasing trend (0.18 days/year), indicating later freeze-up, and a decreasing trend (−0.05 days/year), revealing earlier break-up.

Spatial trends and distribution of LIT and LIP of a given lake can also be analyzed. Random years and dates were selected to demonstrate this on Agassiz Lake (Figures 5d–5i). Ice thickness distribution on Agassiz Lake for 22 May 1990, and 2000 is shown in Figures 5d and 5e, respectively. LIT distribution ranged from 100 to 117 cm on 22 May 1990, and 0–16 cm on the same day of the year in 2000. The freeze-up and break-up trend on the lake for a given year, showing the day and location, can be retrieved from the simulated data. An example of freeze-up distribution is shown for Agassiz Lake for 2011(Figure 5f) and 2022 (Figure 5g). Break-up distribution is also seen for 1992 (Figure 5h) and 2009 (Figure 5i).

3.3. Comparative Analysis of Lake Ice Thickness and Phenology: 1991–1992 Versus 2021–2022

3.3.1. Lake Ice Thickness

Figures 6a and 6b show the spatial distribution of LIT for 1991 to 1992 (historical) and 2021 to 2022 (recent) ice cover seasons in the NSR. For both seasons, lakes surrounding Yellowknife typically exhibited lower ice thickness than those in other regions. The seasonal mean LIT distribution for the recent ice season ranged from 65 to 90 cm across the NSR. Most lakes (205, or 41%) had mean ice thickness between 70 and 75 cm, with the next group (195, or 39%) exhibiting ice thickness ranging from 65 to 70 cm. Only a few lakes (8, or 1.6%) had ice thickness greater than 80 cm.

Comparing the recent ice season (2021–2022) to 30 years ago (1991–1992) reveals different LIT distributions and patterns. In contrast to the recent season, there were no lakes with ice thickness less than 71 cm in 1991–1992. The distribution of LIT for the 1991–1992 ice season ranged from 71 to 93 cm. The majority of lakes (347, or 69%) had mean ice thickness between 75 and 85 cm. Additionally, 56% of study lakes had ice thickness greater than

10.1029/2025WR040216

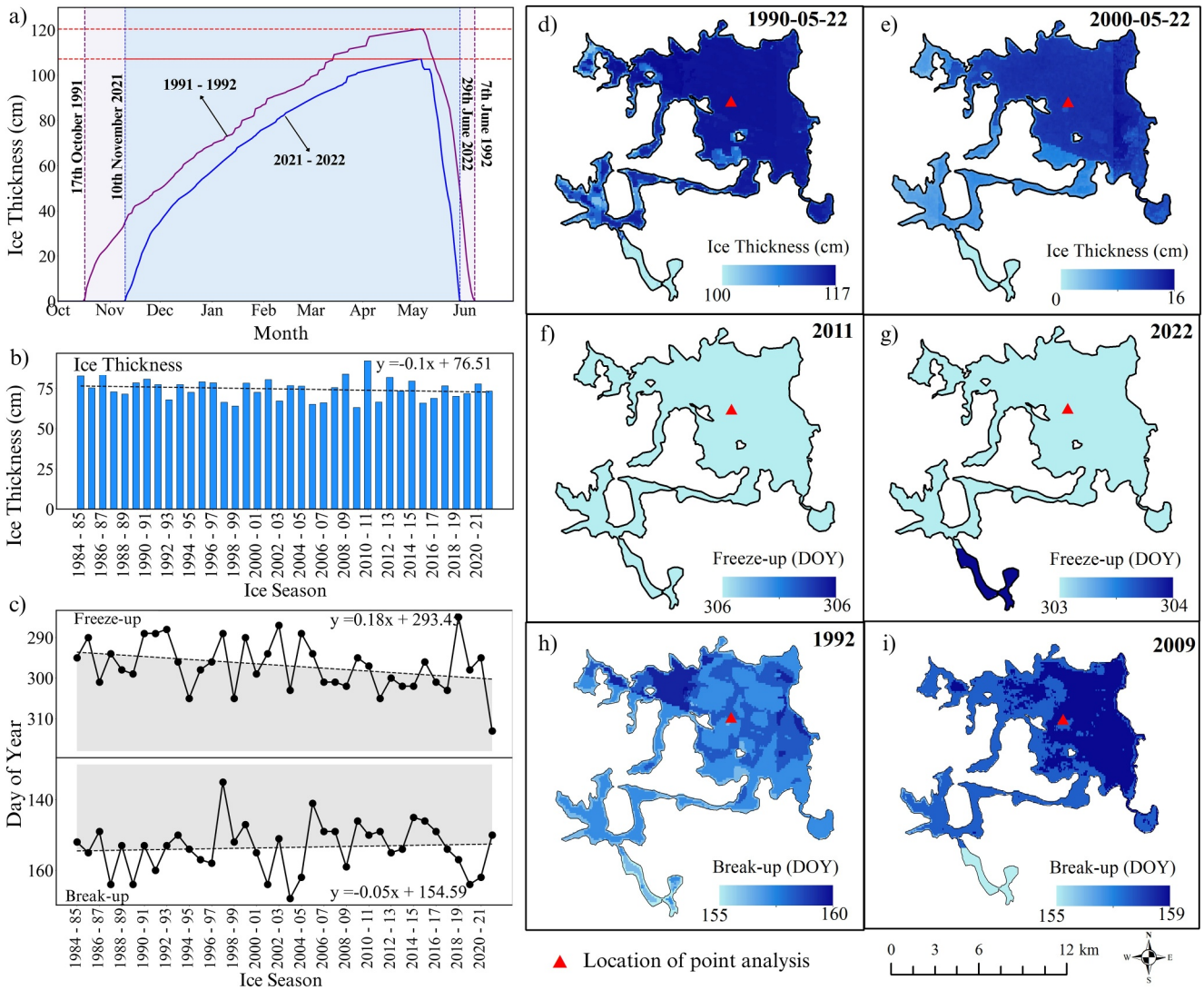

Figure 5. Sample of model output for a chosen lake and time period. (a) Daily Lake ice thickness (LIT) for Agassiz Lake for 1991–1992 and 2021–2022; (b) Yearly mean LIT from 1984 to 2022; (c) Yearly Freeze-up and break-up day from 1984 to 2022. Distribution of LIT for May 22 for (d) 1990 and (e) 2000. Freeze-up distribution for (f) 2011 and (g) 2022; break-up distribution for (h) 1992 and (i) 2009. Color bars are tailored to each image.

80 cm. The results highlighted a significant reduction in LIT in the recent season compared to the previous. A specific comparison of the distribution values of the mean LIT for both seasons is presented in Figure 6c.

3.3.2. Lake Ice Cover Duration

Figures 7a and 7b show the spatial distribution of ICD for the 1991 to 1992 and 2021 to 2022 ice seasons in the NSR. Additionally, a histogram comparing the ICD distribution for both seasons is presented in Figure 7c. Ice cover duration across the region for the 2021 to 2022 ice cover season ranged from 159 to 230 days (Figure 7b) and is widely distributed and very variable. On the other hand, the 1991 to 1992 season saw ICD ranging from 194 to 263 days on lakes across the NSR. There is a shift from longer to shorter ice cover periods, comparing the previous and recent seasons. Lakes with shorter ICD are typically found around Yellowknife; this pattern does not change over the years.

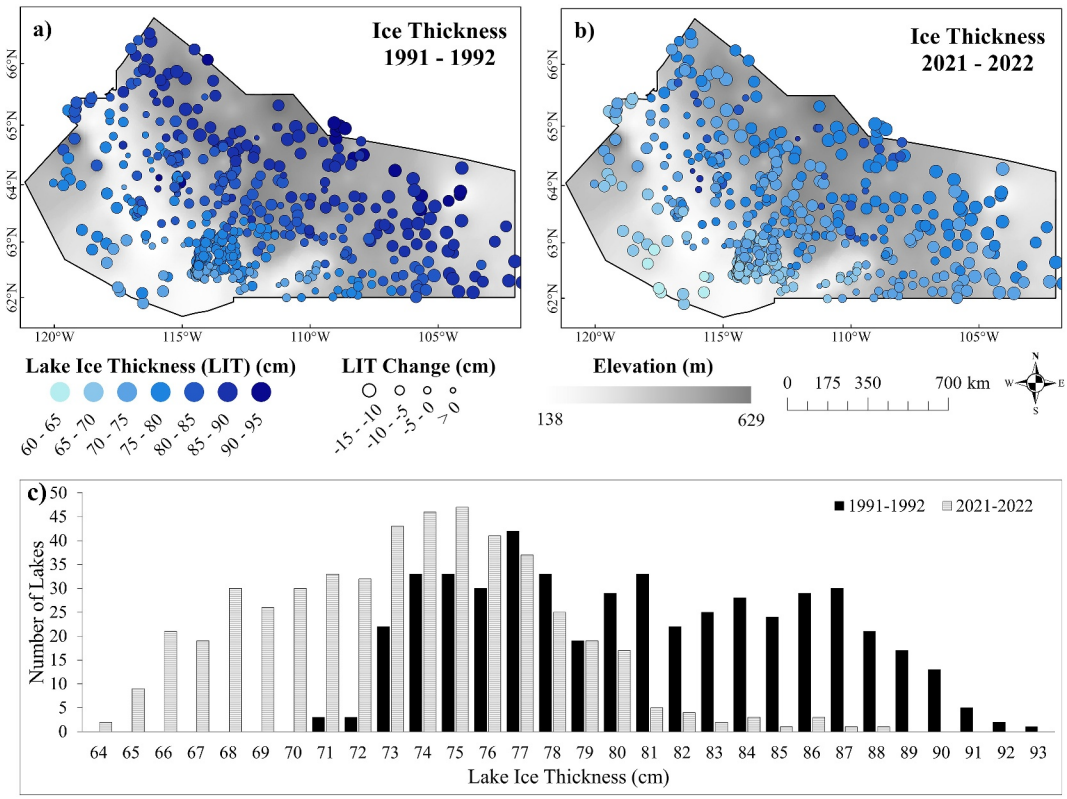

Figure 6. Comparison of the spatial distribution of mean lake ice thickness for (a) 1991–1992 and (b) 2021–2022 ice cover season for study lakes and (c) a histogram showing the distribution of ice thickness among study lakes for the two seasons.

3.4. Trends in Lake Ice Thickness and Ice Cover Duration

3.4.1. Spatial Lake Ice Thickness and Ice Cover Duration Trend

Linear trend analysis revealed substantial heterogeneity in LIT and ice cover trends across lakes in the study region from 1984 to 2022. Over the past four decades, model simulations showed that LIT experienced a statistically significant ($p < 0.05$) reduction. However, the magnitude of ice thickness change is lake-specific and differs across the region, ranging from −0.26 cm/year to −0.10 cm/year (Figure 8). The results found that 323 lakes (65%) had significantly decreased ice thickness. Most lakes (200, or 61.9%) showed a reduction ranging from 0.18/year to 0.15 cm/year (Figure 8b). All 13 lakes with reduction greater than 0.22 cm/year, the highest range, were found in the Northwest of the NSR. Lakes located in low-elevation areas did not show a significant decrease in ice thickness (Figure 8a).

Results revealed that over 63% (309) of lakes had a statistically significant reduction in ICD (the period from the beginning of ice formation till the last day of melt) from 1984 to 2022 (Figure 8c). Ice Cover Duration trends across individual lakes ranged from −0.40 days/year to −0.15 days/year. Most lakes (127, or 25%) show a rate of change between −0.32 days/year and −0.28 days/year (Figure 8d).

3.4.2. Temporal Lake Ice Thickness

Distribution of LIT across study lakes showed a shift toward thinner ice (Figure 9a). Ice thickness showed a significant decrease from November to April across all study lakes (Figure 9b). LIT declined at rates ranging from −0.16 cm/year to −0.22 cm/year between November and April from 1984 to 2022. Among all months, January showed the smallest range of anomalies (−10.1 – 8.9 cm), while April had the largest range (−16.1 - 13.6 cm). The highest rates of LIT decline occurred during the early stages (November) and later stages (March and April) of ice formation. Overall, the thickest ice years were observed prior to the 1998–1999 ice cover season.

10.1029/2025WR040216

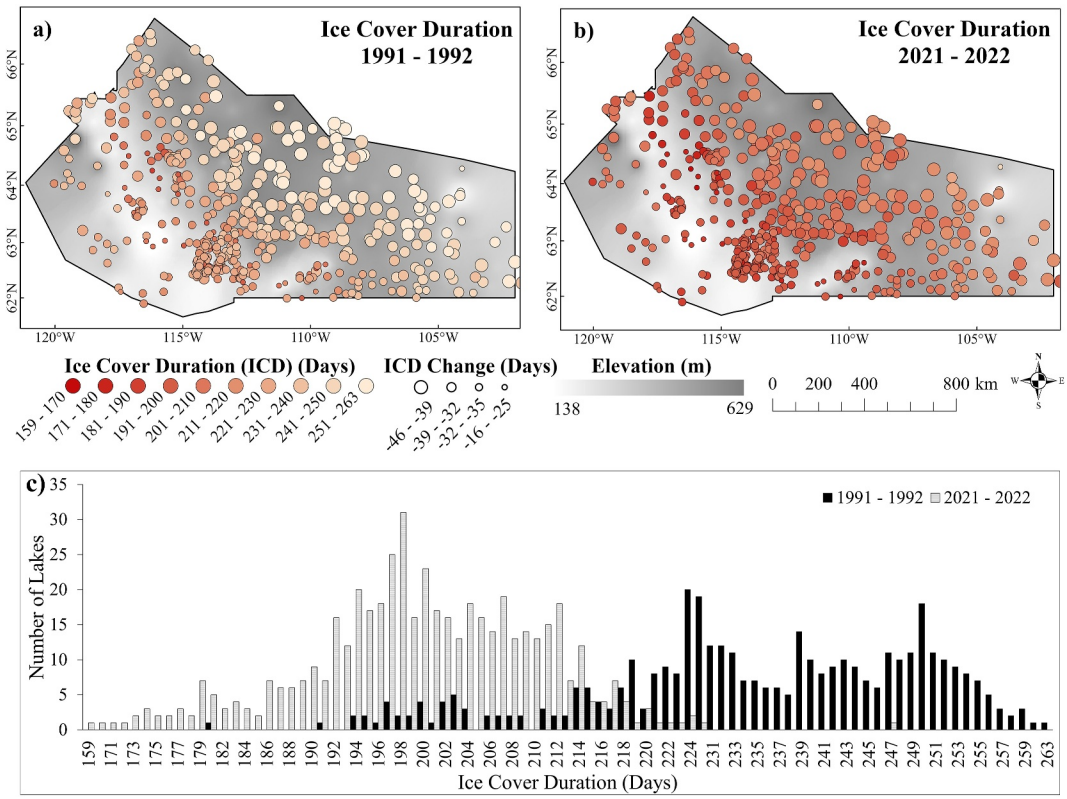

Figure 7. Comparison of the spatial distribution of Ice Cover Duration (ICD) for (a) 1991–1992 and (b) 2021–2022 ice cover season for study lakes and (c) a histogram showing the distribution of ICD among study lakes for the two seasons.

3.5. Relationship Between Ice Cover Distribution, Trends, and Properties

The influence of geographic and morphometric properties on mean LIT, FU, BU and ICD from 1984 to 2022 was examined using a multivariate regression analysis (Table 1). A high proportion of variance was seen across all dependent variables, with overall R^2 values of 0.93 for LIT, 0.95 for FU, 0.98 for BU, and 0.96 for ICD. Latitude (2.78, partial $R^2 = 0.79$, $r = 0.64$), longitude (0.65, partial $R^2 = 0.75$, $r = 0.35$), and Depth (0.25, partial $R^2 = 0.66$, $r = 0.54$) were the strongest predictors of LIT, with deeper lakes and those located further north and east exhibiting thicker ice cover. Lake area exerted a more minor but positive effect (0.01), while elevation and volume had relatively minor influences. Depth overwhelmingly dominates FU timing (1.51 days/m, partial $R^2 = 0.93$, $r = 0.87$), explaining nearly all of the variance compared to other predictors.

BU, on the other hand, was strongly climate and geographically driven. Latitude (5.36 days/°N, partial $R^2 = 0.92$, $r = 0.52$) and longitude (1.59 days/°E, partial $R^2 = 0.94$, $r = 0.61$) had the most potent effects, indicating that the northern and more easterly lakes in the NSR breakup later. Elevation also delayed break-up (0.01 days/m, partial $R^2 = 0.36$, $r = 0.70$). For ICD mean depth was the dominant negative predictor (−1.54 days/m, partial $R^2 = 0.91$, $r = -0.59$), indicating that deep lakes had shorter ICD because they froze later and melted earlier. However, Latitude (8.9 days/°N, partial $R^2 = 0.84$, $r = 0.23$) and longitude (2.68 days/°E,partial $R^2 = 0.87$, $r = 0.57$) also had some influences on ICD.

In addition, the correlation between LIT and ICD trends and geographic and morphometric properties was calculated. Both climatic gradients and lake morphometry strongly shaped trends in LIP and LIT. LIT trend was most strongly correlated with depth ($r = 0.70$, $p < 0.001$), indicating that deeper lakes are thinning faster over time. Freeze-up (FU) trend was also positively correlated with depth ($r = 0.62$), showing that deeper lakes are trending toward later freeze-up. Break-up trend, however, showed a strong negative correlation with latitude ($r = -0.68$), showing that northern lakes within the NSR are shifting toward earlier break-up.

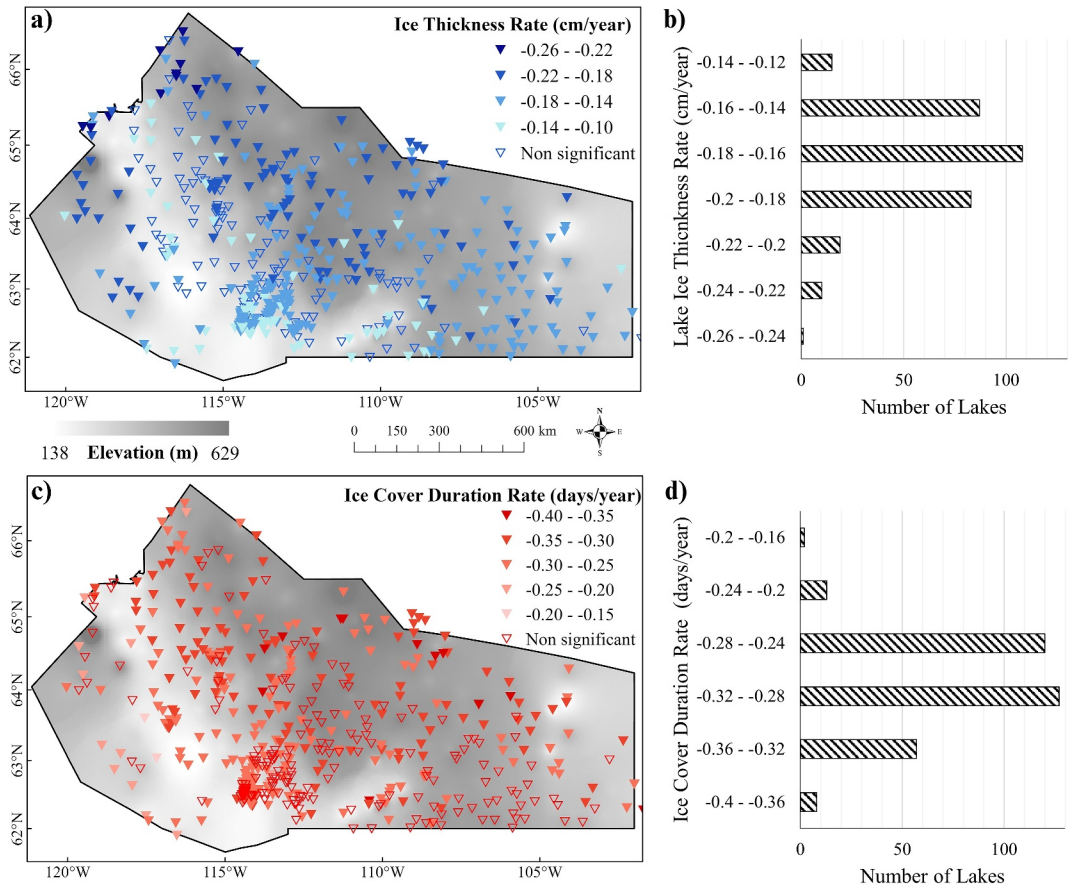

Figure 8. (a) Rate of lake ice thickness (LIT) change on all study lakes from 1984 to 2022; (b) distribution of LIT rate of change; (c) rate of ice cover duration (ICD) change on all study lakes from 1984 to 2022; (d) distribution of ICD rate of change.

4. Discussion

4.1. Advancement in Spatially Distributed Modeling of Lake Ice

This study adapted and distributed CLIMo, a 1-D thermodynamic lake ice model, to operate at a 50 m (~0.0005°) resolution for small to medium-sized lakes using North Slave LST, ERA5-Land and ERA5 data as input. This spatially distributed approach integrates satellite-derived North Slave LST and ERA5/ERA5-Land reanalysis products. The model's performance across 500 diverse lakes in NSR demonstrates the utility of high-resolution, spatially explicit data in capturing both LIT and LIP. The model achieved an RMSE of 2.7–7 cm compared to in situ measurements and a similarly strong agreement with SIMBA data. These results underscore how spatially resolved forcing and finer-scale physical parameterizations can meaningfully improve the fidelity of lake ice simulations.

4.2. Drivers and Trends of Lake Ice Variability

Our model simulations from 1984 to 2022 show a marked decline in LIT (−0.26 to −0.10 cm/year) and a shortening of ICD (−0.40 to −0.15 days/year) across most studied lakes. This trend aligns with other high-latitude investigations (e.g., Brown & Duguay, 2011; Dibike et al., 2011) that attribute lake ice loss to rising air temperatures, changes in snow regimes, and large-scale atmospheric circulation patterns. This decline in LIT may be linked to the recent increase in winter air temperatures and precipitation in the region recorded at the Yellowknife weather station between 1998 and 2022, contributing to deeper snow accumulation. Deeper snow depths likely inhibit downward ice growth through enhanced insulation, a phenomenon noted in previous studies (Gao & Stefan, 2004; Morris & Duguay, 2005).

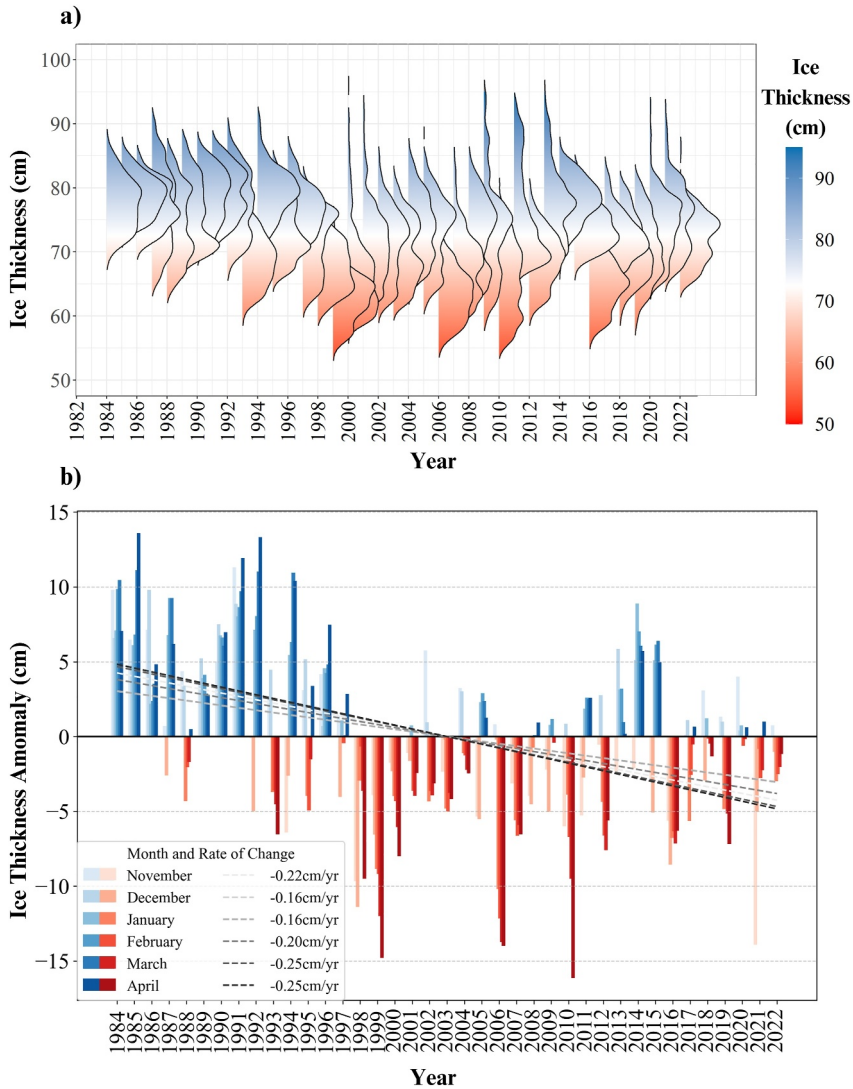

Figure 9. (a) Distribution of Lake Ice Thickness (LIT) across study lakes from 1984 to 2022, (b) monthly anomalies and rate of change in LIT from 1984 to 2022. The gray dashed lines represent the trend lines for each month.

Furthermore, ice thickness anomalies in this study show a clear shift beginning around the 1997–1998 period, which coincides with an El Niño event (Bonsal et al., 2006). El Niño years are characterized by warmer-than-average winter temperatures in northern regions, including the NSR, and can bring milder conditions with increased snowfall due to higher moisture availability. Such conditions contribute to thinner lake ice and shorter ice cover seasons. Research has shown that El Niño years can shorten lake ice seasons by up to 10 days (Bonsal et al., 2006).

Seasonally, the most rapid LIT declines occurred in early winter (November) and spring (March to April). These transitions are highly sensitive to warming air temperatures and higher solar radiation, which reinforce a positive feedback loop: thinner autumn ice facilitates prolonged open-water conditions that enhance heat absorption and delay freeze-up; conversely, in spring, thinner ice melts more quickly, driving earlier break-up and thus shortening ICD (Huang et al., 2022). Given that much of subarctic Canada experiences warming rates exceeding global averages (Larsen et al., 2014; Rantanen et al., 2022), continued acceleration of these ice losses seems probable unless substantial climate-mitigating measures are taken.

Table 1
Multilinear Regression of Mean Lake Ice Thickness (LIT), Freeze-Up (FU), Break-Up (BU), and Ice Cover Duration (ICD) From 1984 to 2022 Against Lake Morphometry and Geographic Predictors

Dependent variable	Predictor	Coefficient (standard error)	Correla-tion	Partial R^2	VIF	R^2	Model *p*-value
Lake Ice Thickness (LIT) - cm	Latitude (°)	2.78 (0.07)	0.64[a]	0.79	1.74	0.93	<0.001
	Longitude (°)	0.65 (0.02)	0.35[a]	0.75	1.61		
	Elevation (m)	0.00 (0.00)	0.56[a]	0.03	1.66		
	Area (km^2)	0.01 (0.00)	0.29[a]	0.06	7.34		
	Depth (m)	0.25 (0.01)	0.54[a]	0.66	1.42		
	Volume (km^3)	−0.00 (0.00)	0.27[a]	0.07	8.04		
Freeze-up (FU) - DOY	Latitude (°)	−3.55 (0.15)	0.03	0.54	1.74	0.95	<0.001
	Longitude (°)	−1.09 (0.04)	−0.38[a]	0.62	1.61		
	Elevation (m)	−0.01 (0.00)	−0.28[a]	0.10	1.66		
	Area (km^2)	0.02 (0.00)	0.23[a]	0.08	7.34		
	Depth (m)	1.51 (0.02)	0.87[a]	0.93	1.42		
	Volume (km^3)	−0.00 (0.00)	0.34[a]	0.10	8.04		
Break-up (BU) - DOY	Latitude (°)	5.36 (0.07)	0.52[a]	0.92	1.74	0.98	<0.001
	Longitude (°)	1.59 (0.02)	0.61[a]	0.94	1.61		
	Elevation (m)	0.01 (0.00)	0.70[a]	0.36	1.66		
	Area (km^2)	0.01 (0.00)	0.21[a]	0.07	7.34		
	Depth (m)	−0.03 (0.01)	0.10[b]	0.03	1.42		
	Volume (km^3)	−0.00 (0.00)	0.13[c]	0.02	8.04		
Ice Cover Duration (ICD) - Days	Latitude (°)	8.91 (0.18)	0.23[a]	0.84	1.74	0.96	<0.001
	Longitude (°)	2.68 (0.05)	0.57[a]	0.87	1.61		
	Elevation (m)	0.02 (0.00)	0.54[a]	0.25	1.66		
	Area (km^2)	−0.01 (0.00)	−0.06	0.02	7.34		
	Depth (m)	−1.54 (0.02)	−0.59[a]	0.91	1.42		
	Volume (km^3)	0.00 (0.00)	−0.18[a]	0.05	8.04		

[b]$p < 0.05$. [c]$p < 0.01$. [a]$p < 0.001$.

4.3. Influence of Morphometry and Geographic Factors

Our correlation analysis revealed that lake depth predominantly controls freeze-up dates, duration of ice and in combination with latitude/longitude, ice thickness, while geographic variables (latitude and elevation) more strongly influence break-up timing. Deeper lakes require longer periods to cool and form stable ice covers, thus exhibiting later freeze-up (Williams & Stefan, 2006). However, break-up appears more sensitive to broad-scale climate gradients such as cooler, higher-elevation environments that preserve ice longer in spring.

These findings highlight the heterogeneity in lake ice responses, even across a relatively bounded region such as the NSR, and reflect the need for lake-specific modeling. Ignoring local morphometric properties can underestimate the spatial complexity of ice processes (Arp et al., 2013; Liston & Dorothy, 1995). Future studies may benefit from improved high-resolution bathymetry data or coupling thermodynamic models with three-dimensional hydrodynamic models to examine vertical mixing processes that can further modulate freeze-up and break-up.

4.4. Ecological and Socioeconomic Implications

The observed decreases in LIT and ICD have significant consequences for both local ecosystems and communities. Reduced ice cover alters the thermal regime, with cascading effects on nutrient cycling, primary productivity, and oxygen availability (Hampton et al., 2017; Weyhenmeyer et al., 2022). Earlier break-up can intensify surface warming, leading to earlier and potentially more pronounced summer stratification (Smucker

et al., 2021). Such shifts can disrupt established food webs and increase greenhouse gas emissions from lakes (Woolway et al., 2020).

From a socioeconomic perspective, the NSR relies on ice roads for resource extraction (e.g., diamond mining) and community connectivity. Declining LIT, particularly if it falls below recommended safe thresholds (Perrin et al., 2015), jeopardizes transportation networks such as the Tibbitt TCWR, potentially driving up costs for freight and limiting access to remote regions (Mullan et al., 2017). These climate-driven changes thus pose challenges not only to environmental management but also to regional infrastructure, cultural traditions, and economic viability.

4.5. Limitations and Future Directions

The primary limitation in this modeling effort is the reliance on relatively coarse (~30 km) ERA5 data for atmospheric variables. While this study successfully integrated a higher-resolution (~30 m) satellite-based LST, finer-scale meteorological forcing (e.g., from downscaled reanalyzes or region-specific weather models) could further refine estimates of local air temperature, precipitation, and wind fields. Enhanced resolution of spatial snow distribution data is essential (Pouw et al., 2023), as it removes the necessity of relying on a fixed snow retention scenario value (75%) used in the study, which influences the spatial heterogeneity of ice thickness as well as the values themselves, due to snow's insulating properties. Furthermore, detailed information on snow and lake bathymetry is vital, as these factors significantly affect the processes of ice formation and melt.

This model focuses on thermodynamic processes and does not explicitly account for dynamic factors like wind-driven ice redistribution, ice rafting, or snow drifting, which could introduce local heterogeneity in ice thickness. Essentially, this is a spatially distributed 1D model with no coupling between neighboring model grid cells, and thus horizontal heat fluxes are not represented. Incorporating such processes is a valuable direction for future model development. Further work could also integrate remote-sensing-derived snow-on-ice products, LiDAR-based snow depth retrievals, or coupling with hydrodynamic models for more comprehensive representations of under-ice processes.

5. Conclusions

This study successfully applied a spatially distributed one-dimensional thermodynamic model to simulate LIT and lake LIP at a fine resolution (~50 m) across 500 predominantly small to medium-sized lakes in the NSR, NWT, Canada. By integrating satellite-derived (North Slave LST) and ERA5 reanalysis data, the model captured spatial and temporal variations in ice thickness, freeze-up, and break-up dates. Validation against field-based measurements and SIMBA observations showed good agreement, underscoring the potential of distributed modeling in regions with limited in situ data.

The results revealed a significant shift in lake ice conditions comparing the 1991–1992 and 2021–2022 ice seasons, characterized by thinner ice, later freeze-up, earlier break-up, and shorter ICD. Over the 1984 to 2022 period, 65% of the lakes exhibited a significant decline in LIT, while 63% showed significantly reduced ICD. Monthly analyses confirmed consistent negative trends in LIT (−0.16 to −0.24 cm/yr), highlighting the strong influence of changing winter conditions. Further correlation analyses suggested that morphometric attributes (e.g., depth) exert a stronger control on ICD and freeze-up processes, whereas geographic factors (e.g., latitude and elevation) play a more significant role in determining break-up timing.

These findings have critical implications for local communities, industries, and ecosystems. Declining ice thickness not only compromises winter transportation routes, which are vital for resource extraction and community connectivity, but also accelerates lake warming, alters mixing regimes, and potentially impacts aquatic habitats and regional hydrological processes. The data generated through this study present valuable resources for forecasting and managing the ecological and socioeconomic repercussions of changing ice dynamics. Future research can build on this approach by incorporating more detailed bathymetric data, higher-resolution meteorological inputs, and explicit ice–snow feedback mechanisms. This will enable more comprehensive and robust modeling of lake ice processes, further supporting adaptation efforts in northern regions.

Data Availability Statement

The daily lake ice thickness and yearly phenology records for the study lakes in the North Slave region are published under the DOI: https://doi.org/10.5683/SP3/2FZY9M (Attiah et al., 2025). The data set includes tab files for each lake, showing mean, maximum and minimum daily ice thickness, yearly break-up and freeze-up distribution. The lake ice model builds on code that is externally owned and therefore cannot be publicly archived, but the code may be shared in consultation with the code owner. Physical properties and names of lakes were derived from HydroLAKES (https://www.hydrosheds.org/products/hydrolakes, HydroSheds, 2022; Messager et al., 2016), Water File –Lakes and Rivers (polygons) data (https://open.canada.ca/data/en/dataset/d0cdef71-9343-46c3-b2e7-c1ded5907686, Statistics Canada, 2022) and CanVec Series (https://open.canada.ca/data/en/dataset/9d96e8c9-22fe-4ad2-b5e8-94a6991b744b; Natural Resources Canada, 2023) which contains information licensed under the Open Government Licence—Canada. ERA5 reanalysis data were obtained from Copernicus Climate Change Service (https://doi.org/10.24381/cds.adbb2d47; Hersbach et al., 2023), as well as ERA5-Land (https://doi.org/10.24381/cds.e2161bac; Sabater, 2019).

Acknowledgments

The authors respectfully acknowledge that this research was conducted on the traditional lands of the Yellowknives Dene First Nation, within the Chief Drygeese territories. They express their gratitude to the Indigenous Peoples for the opportunity to learn from and carry out fieldwork on their lands. This study was supported by funding from the Natural Sciences and Engineering Research Council of Canada (NSERC) through the Canada Research Chair (CRC) program and the NSERC Discovery Grant (RGPIN-2020-05573) awarded to Kheyrollah Pour. Additional support was provided by the Canada Excellence Research Chair—Global Water Futures (CERC-GWF) initiative under the Remotely Sensed Monitoring of Northern Lake Ice project (Grant 353374), as well as the Government of the NWT, Environment and Climate Change, and the Cumulative Impact Monitoring Program (CIMP-212). Computational resources for this research were made possible through Compute Ontario (https://www.computeontario.ca/, last accessed: 1 February 2025) and the Digital Research Alliance of Canada (https://alliancecan.ca/en, last accessed: 1 February 2025).

References

Arp, C. D., Jones, B. M., & Grosse, G. (2013). Recent lake ice-out phenology within and among lake districts of Alaska, U.S.A. *Limnology & Oceanography*, *58*(6), 2013–2028. https://doi.org/10.4319/lo.2013.58.6.2013

Attiah, G., Kheyrollah Pour, H., & Scott, K. A. (2022). North Slave Lake surface temperature. https://doi.org/10.5683/SP3/J4GMC2

Attiah, G., Kheyrollah Pour, H., & Scott, K. A. (2023a). Four decades of lake surface temperature in the Northwest Territories, Canada, using a lake-specific satellite-derived dataset. *Journal of Hydrology: Regional Studies*, *50*, 101571. https://doi.org/10.1016/j.ejrh.2023.101571

Attiah, G., Kheyrollah Pour, H., & Scott, K. A. (2023b). Lake surface temperature retrieved from Landsat satellite series (1984 to 2021) for the North Slave Region. *Earth System Science Data*, *15*(3), 1329–1355. https://doi.org/10.5194/essd-15-1329-2023

Attiah, G., Scott, K. A., & Kheyrollah Pour, H. (2025). North Slave Lake Ice Thickness and Phenology retrieved from a thermodynamic model, 1984 to 2022. *Borealis, V1*. https://doi.org/10.5683/SP3/2FZY9M

Bonsal, B. R., Prowse, T. D., Duguay, C. R., & Lacroix, M. P. (2006). Impacts of large-scale teleconnections on freshwater-ice break/freeze-up dates over Canada. *Journal of Hydrology*, *330*(1–2), 340–353. https://doi.org/10.1016/j.jhydrol.2006.03.022

Brown, L. C., & Duguay, C. R. (2010). The response and role of ice cover in lake-climate interactions. *Progress in Physical Geography*, *34*(5), 671–704. https://doi.org/10.1177/0309133310375653

Brown, L. C., & Duguay, C. R. (2011). A comparison of simulated and measured lake ice thickness using a Shallow Water Ice Profiler. *Hydrological Processes*, *25*(19), 2932–2941. https://doi.org/10.1002/hyp.8087

Cruikshank, D. R. (1984). *The relationship of summer thermocline depth to several physical characteristics of lakes. Western Region*. Department of Fisheries and Oceans.

Dastour, H., Ghaderpour, E., & Hassan, Q. K. (2022). A Combined Approach for Monitoring Monthly Surface Water/Ice Dynamics of Lesser Slave Lake Via Earth Observation Data. *Ieee Journal of Selected Topics in Applied Earth Observations and Remote Sensing*, *15*, 6402–6417. https://doi.org/10.1109/JSTARS.2022.3196611

Dibike, Y., Prowse, T., Saloranta, T., & Ahmed, R. (2011). Response of Northern Hemisphere lake-ice cover and lake-water thermal structure patterns to a changing climate. *Hydrological Processes*, *25*(19), 2942–2953. https://doi.org/10.1002/hyp.8068

Duguay, C. R., Flato, G. M., Jeffries, M. O., Ménard, P., Morris, K., & Rouse, W. R. (2003). Ice-cover variability on shallow lakes at high latitudes: Model simulations and observations. *Hydrological Processes*, *17*(17), 3465–3483. https://doi.org/10.1002/hyp.1394

Gao, S., & Stefan, H. G. (2004). Potential Climate Change Effects on Ice Covers of Five Freshwater Lakes. *Journal of Hydrologic Engineering*, *9*(3), 226–234. https://doi.org/10.1061/(asce)1084-0699(2004)9:3(226)

Guo, L., Zheng, H., Wu, Y., Fan, L., Wen, M., Li, J., et al. (2021). An integrated dataset of daily lake surface water temperature over Tibetan Plateau. *Earth System Science Data Discussions*(July), 1–15.

Hampton, S. E., Galloway, A. W. E., Powers, S. M., Ozersky, T., Woo, K. H., Batt, R. D., et al. (2017). Ecology under lake ice. *Ecology Letters*, *20*(1), 98–111. https://doi.org/10.1111/ele.12699

Hampton, S. E., Powers, S. M., Dugan, H. A., Knoll, L. B., McMeans, B. C., Meyer, M. F., et al. (2024). Environmental and societal consequences of winter ice loss from lakes. *Science*, *386*(6718), eadl3211. https://doi.org/10.1126/science.adl3211

Hersbach, H., Bell, B., Berrisford, P., Biavati, G., Horányi, A., Muñoz Sabater, J., et al. (2023). ERA5 hourly data on single levels from 1940 to present. *Copernicus Climate Change Service (C3S) Climate Data Store (CDS)*. https://doi.org/10.24381/cds.adbb2d47

Hersbach, H., Bell, B., Berrisford, P., Hirahara, S., Horányi, A., Muñoz-Sabater, J., et al. (2020). The ERA5 global reanalysis. *Quarterly Journal of the Royal Meteorological Society*, *146*(730), 1999–2049. https://doi.org/10.1002/qj.3803

Huang, L., Timmermann, A., Lee, S. S., Rodgers, K. B., Yamaguchi, R., & Chung, E. S. (2022). Emerging unprecedented lake ice loss in climate change projections. *Nature Communications*, *13*(1), 5798. https://doi.org/10.1038/s41467-022-33495-3

Huss, M., & Farinotti, D. (2012). Distributed ice thickness and volume of all glaciers around the globe. *Journal of Geophysical Research*, *117*(4), 1–10. https://doi.org/10.1029/2012JF002523

Kämäri, M., Alho, P., Colpaert, A., & Lotsari, E. (2017). Spatial variation of river-ice thickness in a meandering river. *Cold Regions Science and Technology*, *137*, 17–29. https://doi.org/10.1016/j.coldregions.2017.01.009

Kendall, M. G. (1975). *Rank correlation methods. 4th edition*. Charles Griffin.

Kheyrollah Pour, H., Attiah, G., Thompson, J., Scott, K. A., & Duguay, C. (2024). CLIMoGrid v1.0: A spatially distributed thermodynamic lake ice model 2. Retrieved from https://ssrn.com/abstract=4979507

Knoll, L. B., Sharma, S., Denfeld, B. A., Flaim, G., Hori, Y., Magnuson, J. J., et al. (2019). Consequences of lake and river ice loss on cultural ecosystem services. *Limnology And Oceanography Letters*, *4*(5), 119–131. https://doi.org/10.1002/lol2.10116

Larsen, J. N., Anisimov, O. A., Constable, A., Hollowed, A. B., Maynard, N., Prestrud, P., et al. (2014). Polar regions. In *Climate change 2014: Impacts, adaptation and Vulnerability: Part B: Regional aspects: Working group II contribution to the fifth assessment report of the Intergovernmental Panel on climate change (Issue January)*. https://doi.org/10.1017/CBO9781107415386.008

Lehnherr, I., St Louis, V. L., Sharp, M., Gardner, A. S., Smol, J. P., Schiff, S. L., et al. (2018). The world's largest High Arctic lake responds rapidly to climate warming. *Nature Communications*, *9*(1), 1–9. https://doi.org/10.1038/s41467-018-03685-z

Liston, G., & Dorothy, H. (1995). An energy-balance model of lake-ice evolution.

Matsumoto, M., Yoshimura, M., Naoki, K., Cho, K., & Wakabayashi, H. (2019). Ground penetrating radar data interpretation using electromagnetic field analysis for sea ice thickness measurement. *International Archives of the Photogrammetry, Remote Sensing and Spatial Information Sciences–ISPRS Archives*, *42*(3/W7), 47–50. https://doi.org/10.5194/isprs-archives-XLII-3-W7-47-2019

Ménard, P., Duguay, C. R., Flato, G. M., & Rouse, W. R. (2002). Simulation of ice phenology on Great Slave Lake, Northwest Territories, Canada. *Hydrological Processes*, *16*(18), 3691–3706. https://doi.org/10.1002/hyp.1230

Messager, M. L., Lehner, B., Grill, G., Nedeva, I., & Schmitt, O. (2016). Estimating the volume and age of water stored in global lakes using a geostatistical approach. *Nature Communications*, *7*, 1–11. https://doi.org/10.1038/ncomms13603

Morris, J. M., & Duguay, C. (2005). Model simulation of the effects of climate variability and change on lake ice in central Alaska, USA. *Annals of Glaciology*, *40*, 113–118. https://doi.org/10.3189/172756405781813663

Mullan, D., Swindles, G., Patterson, T., Galloway, J., Macumber, A., Falck, H., et al. (2017). Climate change and the long-term viability of the World's busiest heavy haul ice road. *Theoretical and Applied Climatology*, *129*(3–4), 1089–1108. https://doi.org/10.1007/s00704-016-1830-x

O'Reilly, C. M., Rowley, R. J., Schneider, P., Lenters, J. D., Mcintyre, P. B., & Kraemer, B. M. (2015). Rapid and highly variable warming of lake surface waters around the globe. *Geophysical Research Letters*, *42*, 1–9. https://doi.org/10.1002/2015GL066235.Received

Perrin, A., Dion, J., Eng, S., Sawyer, D., Nodelman, J. Y. H. J. R., Comer, N., et al. (2015). Economic Implications of Climate Change: Adaptations of mine access roads in northern Canada. *Iisd*, *93*. https://www.iisd.org/project/economic-implications-climate-change-adaptations-mine-access-roads-northern-canada%0Ahttp://files/13/economic-implications-climate-change-adaptations-mine-access-roads-northern-canada.html

Persson, P. O. G., Fairall, C. W., Andreas, E. L., Guest, P. S., & Perovich, D. K. (2002). Measurements near the Atmospheric Surface Flux Group tower at SHEBA: Near-surface conditions and surface energy budget. *Journal of Geophysical Research*, *107*(10), 1–35. https://doi.org/10.1029/2000jc000705

Post, E., Alley, R. B., Christensen, T. R., Macias-Fauria, M., Forbes, B. C., Gooseff, M. N., et al. (2019). The polar regions in a 2°C warmer world. *Science Advances*, *5*(12), eaaw9883. https://doi.org/10.1126/sciadv.aaw9883

Pouw, A. F., Kheyrollah Pour, H., & MacLean, A. (2023). Mapping snow depth on Canadian sub-arctic lakes using ground-penetrating radar. *The Cryosphere*, *17*(6), 2367–2385. https://doi.org/10.5194/tc-17-2367-2023

Prowse, T., Alfredsen, K., Beltaos, S., Bonsal, B. R., Bowden, W. B., Duguay, C. R., et al. (2011). Effects of changes in arctic lake and river ice. *Ambio*, *40*(1), 63–74. https://doi.org/10.1007/s13280-011-0217-6

Prowse, T. D., Furgal, C., Chouinard, R., Melling, H., Milburn, D., & Smith, S. L. (2009). Implications of climate change for economic development in Northern Canada: Energy, resource, and transportation sectors. *Ambio*, *38*(5), 272–281. https://doi.org/10.1579/0044-7447-38.5.272

Qiu, Y., Xie, P., Leppäranta, M., Wang, X., Lemmetyinen, J., Lin, H., & Shi, L. (2019). MODIS-based Daily Lake Ice Extent and Coverage dataset for Tibetan Plateau. *Big Earth Data*, *3*(2), 170–185. https://doi.org/10.1080/20964471.2019.1631729

Rafat, A., Kheyrollah Pour, H., Spence, C., Palmer, M. J., & MacLean, A. (2023). An analysis of ice growth and temperature dynamics in two Canadian subarctic lakes. *Cold Regions Science and Technology*, *210*(2022), 103808. https://doi.org/10.1016/j.coldregions.2023.103808

Rantanen, M., Karpechko, A. Y., Lipponen, A., Nordling, K., Hyvärinen, O., Ruosteenoja, K., et al. (2022). The Arctic has warmed nearly four times faster than the globe since 1979. *Communications Earth & Environment*, *3*(1), 168. https://doi.org/10.1038/s43247-022-00498-3

Sabater, M. (2019). ERA5-Land hourly data from 1950 to present. *Copernicus Climate Change Service (C3S) Climate Data Store (CDS)*. https://essd.copernicus.org/articles/13/4349/2021/essd-13-4349-2021.html

Slater, T., Lawrence, I. R., Otosaka, I. N., Shepherd, A., Gourmelen, N., Jakob, L., et al. (2021). Review article: Earth's ice imbalance. *The Cryosphere*, *15*(1), 233–246. https://doi.org/10.5194/tc-15-233-2021

Šmejkalová, T., Edwards, M. E., & Dash, J. (2016). Arctic lakes show strong decadal trend in earlier spring ice-out. *Scientific Reports*, *6*, 1–8. https://doi.org/10.1038/srep38449

Smucker, N. J., Beaulieu, J. J., Nietch, C. T., & Young, J. L. (2021). Increasingly severe cyanobacterial blooms and deep water hypoxia coincide with warming water temperatures in reservoirs. *Global Change Biology*, *27*(11), 2507–2519. https://doi.org/10.1111/gcb.15618

Spence, C., Blanken, P. D., Hedstrom, N., Fortin, V., & Wilson, H. (2011). Evaporation from Lake Superior: 2. Spatial distribution and variability. *Journal of Great Lakes Research*, *37*(4), 717–724. https://doi.org/10.1016/j.jglr.2011.08.013

Wang, W., Lee, X., Xiao, W., Liu, S., Schultz, N., Wang, Y., et al. (2018). Global lake evaporation accelerated by changes in surface energy allocation in a warmer climate. *Nature Geoscience*, *11*(6), 410–414. https://doi.org/10.1038/s41561-018-0114-8

Wang, X., Key, J. R., & Liu, Y. (2010). A thermodynamic model for estimating sea and lake ice thickness with optical satellite data. *Journal of Geophysical Research*, *115*(12), 1–14. https://doi.org/10.1029/2009JC005857

Warne, C. P. K., McCann, K. S., Rooney, N., Cazelles, K., & Guzzo, M. M. (2020). Geography and Morphology Affect the Ice Duration Dynamics of Northern Hemisphere Lakes Worldwide. *Geophysical Research Letters*, *47*(12), 1–10. https://doi.org/10.1029/2020GL087953

Weyhenmeyer, G. A., Obertegger, U., Rudebeck, H., Jakobsson, E., Jansen, J., Zdorovennova, G., et al. (2022). Towards critical white ice conditions in lakes under global warming. *Nature Communications*, *13*(1), 4974. https://doi.org/10.1038/s41467-022-32633-1

Williams, S. G., & Stefan, H. G. (2006). Modeling of Lake Ice Characteristics in North America Using Climate, Geography, and Lake Bathymetry. *Journal of Cold Regions Engineering*, *20*(4), 140–167. https://doi.org/10.1061/(asce)0887-381x(2006)20:4(140)

Woolway, R. I., Jennings, E., & Carrea, L. (2020). Impact of the 2018 European heatwave on lake surface water temperature. *Inland Waters*, *10*(3), 322–332. https://doi.org/10.1080/20442041.2020.1712180